Geochimica et Cosmochimica Acta, 1972, Vol. 36, pp. 597 to 619. Pergamon Press. Printed in Northern Ireland

Condensation in the primitive solar nebula

LAWRENCE GROSSMAN
Department of Geology and Geophysics, Yale University, New Haven, Connecticut 06520

(*Received* 5 *August* 1971; *accepted in revised form* 30 *December* 1971)

Abstract—The distribution of the major elements between vapor and solid has been calculated for a cooling gas of cosmic composition. The assumption is made that high temperature condensates remain in equilibrium with the vapor, affecting the temperatures of appearance of successively less refractory phases. The model suggests that the major textural features and mineralogical composition of the Ca, Al-rich inclusions in the C3 chondrites were produced during condensation in the nebula characterized by slight departures from chemical equilibrium due to incomplete reaction of high temperature condensates. Fractionation of such a phase assemblage is sufficient to produce part of the lithophile element depletion of the ordinary chondrites relative to the cosmic abundances.

Iron–nickel alloys have higher condensation temperatures than forsterite and enstatite at all total pressures greater than $7{\cdot}1 \times 10^{-5}$ atmospheres. These data lend support to the origin of the core and mantle of the earth by a heterogeneous accumulation process. The temperature difference between the condensation points of iron and magnesium silicates increases with pressure allowing the possibility of greater fractionation of metal from silicate towards the center of the solar nebula where the pressure and temperature were highest.

INTRODUCTION

ELEMENT fractionations accompanying the condensation of crystalline grains from the primitive solar nebula have undoubtedly been of considerable importance in establishing the distribution of the elements in the interiors of the planets (EUCKEN, 1944; LEWIS, 1969; TUREKIAN and CLARK, 1969; CLARK *et al.*, 1972; GAST, 1972) and between the various meteorite classes (BLANDER and KATZ, 1967; LARIMER, 1967; LARIMER and ANDERS, 1967, 1970; ANDERS, 1968; ARRHENIUS and ALFVÉN, 1971; BLANDER, 1971; KEAYS *et. al.*, 1971). The recognition of this importance of crystal–vapor equilibria has led many workers to attempt to derive the composition of the condensates in equilibrium with the nebular gas over a wide range of pressures and temperatures.

Using Brown's (1949) abundance table, UREY (1952) calculated the stability fields of a number of condensed phases in equilibrium with a gas of solar composition at a pressure of 10^{-2} atm. in which the total gaseous oxygen remaining after condensation of oxides and silicates was assumed to be in the form of H_2O. UREY (1954) performed similar calculations using modified cosmic abundances at gas pressures from 10^{-2} atm. to 10 atm. in a further attempt to predict the loss of volatile elements during the formation of protoplanets. WOOD (1963) derived the pressure–temperature stability fields of solid and liquid iron, forsterite and enstatite in equilibrium with a gas having the composition given by the solar abundance data of GOLDBERG *et al.* (1960).

LORD (1965) performed thermodynamic calculations on the distribution of the elements among their gaseous molecular species using the solar elemental abundances of GOLDBERG *et al.* (1960). He was able to calculate the P_{H_2} required for a number of silicates and oxides to be condensed by the time the gas cooled

to 2000°K and 1700°K. FIX (1970) has reported the results of similar calculations. The purpose of both these investigations was to shed light on the identity of grains in the cool atmospheres of oxygen-rich stars. Using cosmic abundance data primarily from CAMERON (1963a), LARIMER (1967) calculated the sequence of condensation of a wide range of elements and compounds at total pressures of 1 atm and $6{\cdot}6 \times 10^{-3}$ atm by considering the dominant gaseous equilibria. He presented both a slow cooling model which allowed solid solutions to form in complete equilibrium with the nebula by diffusion of end-member components and a fast cooling model which did not. Since no attempt was made by LORD (1965) or LARIMER (1967) to correct the gas composition for the removal of major elements in early condensates, the condensation temperatures are upper limits and the total pressures required for condensation are lower limits for any phase containing an element which has already condensed in a higher temperature mineral.

GILMAN (1969) performed the first full equilibrium calculations where condensate species were included in the mass balance equations for their constituent elements. The gas pressure was 5×10^{-5} atm and its composition was poor in O and Si and rich in Mg, S, Fe, Al and Ca compared to CAMERON's (1968) abundances. This study was aimed at determining the chemical composition of circumstellar condensates of cool oxygen- and carbon-rich stars. LEWIS (1969) presented similar calculations for the pressure–temperature gradient of the atmosphere of Jupiter in an attempt to predict which gaseous compounds would be spectroscopically observable.

The purpose of the present study was to predict what type of chemical fractionation trends would be produced during the equilibrium condensation of grains as the primitive solar nebula cooled. In order to accomplish this, all the optimum features of previous studies were employed. The gas was considered to consist of all the major elements in the proportions given by the most recent solar system abundance table (CAMERON, 1968). All gaseous compounds of these elements for which accurate thermodynamic data could be found were assumed to be present in the system. Care was taken to select a total pressure and an initial temperature consistent with astrophysical models of the primitive inner solar system (CAMERON, 1963b). The vapor was assumed to be in chemical equilibrium with each condensed phase over the entire temperature range between its condensation point and the temperature at which it was consumed by reaction to form new phases. Thus, the derived sequence of condensation is an accurate description of the changing distribution of the elements between vapor and solid phase and between solid phases themselves since the effects of high temperature condensates on the composition of the gas were considered in determining the condensation temperatures of lower temperature species.

METHOD OF CALCULATION

The theory described here is similar to the treatments given by LORD (1965) and LARIMER (1967).

Since H is at least a factor of 10^3 more abundant than every other element except He, which is not considered here, and, since H_2 is always at least a factor of 500 more abundant

than any other H-bearing compound over the temperature range of interest,

$$P_{H_2} \simeq P_{total} \tag{1}$$

where P_{H_2} is the partial pressure of H_2. The total pressure, P_{total}, used in these calculations is 10^{-3} atmospheres. The effects of pressure, temperature and composition gradients and turbulence are ignored in the calculations which follow. From the ideal gas law, which is employed at this low pressure, the density of the gas increases as the temperature decreases, if the pressure is held constant. Then

$$N_{H_2} = P_{H_2}/RT \tag{2}$$

and

$$N_H^{tot} \simeq 2N_{H_2} \tag{3}$$

where N_{H_2} is the number of moles per liter of H_2, R is the gas constant, T is the absolute temperature, and N_H^{tot} is the total number of moles per liter of hydrogen atoms. For any element X

$$N_X^{tot} = \frac{A(X)}{A(H)} \times N_H^{tot} \tag{4}$$

where N_X^{tot} is the number of moles of element X per liter and $A(X)$ and $A(H)$ are the relative abundances of element X and hydrogen, respectively.

For each element in the system, an equation expressing mass balance can be written. In the case of oxygen, for example,

$$N_O + N_{H_2O} + N_{CO} + 2N_{CO_2} + N_{MgO} + \ldots = N_O^{tot}. \tag{5}$$

The initial few sets of calculations are based on 20 such equations, one for each of the 20 most abundant elements, excluding the noble gases. The elements are taken to be present in the proportions given by CAMERON (1968) which are reproduced in Table 1.

ARRHENIUS and ALFVÉN (1971) have shown that even the elements with the lowest ionization potentials will be less than 1 per cent ionized at temperatures below about 2400°K. Since

Table 1. Gaseous species contributing more than 10^{-7} of the total moles of their common constituent element between 2000°K and 1200°K.

Element	Abundance* (Si = 10^6)	Gaseous species
Hydrogen	$2{\cdot}6 \times 10^{10}$	H_2, H, H_2O, HF, HCl, MgH, HS, H_2S, MgOH
Oxygen	$2{\cdot}36 \times 10^7$	CO, SiO, H_2O, TiO, OH, HCO, CO_2, PO, CaO, COS, MgO, SiO_2, AlOH, SO NaOH, MgOH, PO_2, $Mg(OH)_2$, AlO_2H
Carbon	$1{\cdot}35 \times 10^7$	CO, HCN, CS, HCO, CO_2, COS, HCP
Nitrogen	$2{\cdot}44 \times 10^6$	N_2, HCN, PN, NH_3, NH_2
Magnesium	$1{\cdot}05 \times 10^6$	Mg, MgH, MgS, MgF, MgCl, MgO, MgOH, $Mg(OH)_2$
Silicon	$1{\cdot}00 \times 10^6$	Si, SiS, SiO, SiO_2
Iron	$8{\cdot}90 \times 10^5$	Fe
Sulfur	$5{\cdot}06 \times 10^5$	SiS, CS, S, HS, H_2S, PS, AlS, MgS, NS, S_2, COS, SO, CS_2, SO_2
Aluminum	$8{\cdot}51 \times 10^4$	Al, AlH, AlF, AlCl, AlS, AlO, Al_2O, AlOH, AlOF, AlO_2H
Calcium	$7{\cdot}36 \times 10^4$	Ca, CaF, CaO, $CaCl_2$
Sodium	$6{\cdot}32 \times 10^4$	Na, NaH, NaCl, NaF, NaOH
Nickel	$4{\cdot}57 \times 10^4$	Ni
Phosphorus	$1{\cdot}27 \times 10^4$	P, PN, PH, P_2, PH_2, PS, PO, PH_3, PO_2, HCP
Chromium	$1{\cdot}24 \times 10^4$	Cr
Manganese	8800	Mn
Fluorine	3630	HF, AlF, CaF, F, MgF, NaF, NF, KF, PF, CaF_2, AlOF, TiF_2, MgF_2, MgClF, TiF
Potassium	3240	K, KH, KCl, KF, KOH
Titanium	2300	Ti, TiO, TiF_2, TiO_2, TiF
Cobalt	2300	Co
Chlorine	1970	HCl, Cl, AlCl, NaCl, KCl, MgCl, $CaCl_2$, $MgCl_2$, AlOCl, MgClF

* From CAMERON (1968).

the temperature range for condensation at 10^{-3} atmospheres is 1000°K to 1700°K, charged species are ignored in this treatment. Thermodynamic data could be found for 307 gaseous species in this system, with the result that some of the equations had nearly 100 terms in them. It soon became clear that many species were present in such vanishingly small quantities that they would never assume a significant fraction of the total mass of any of their component elements over the entire temperature range of interest (2000°K to 1100°K). These species were removed from the mass balance equations. A further measure of simplification was provided by the fact that each of the elements Fe, Ni, Cr, Mn and Co was present in the vapor phase almost totally as the monatomic species from 2000°K to 1100°K. These 5 elements were removed from the equation set and further calculations with them were performed manually, treating them as an independent subsystem. The system was thus simplified to only 70 gaseous species of 15 elements for the remainder of the calculations. All species considered are listed in Table 1.

Chemical reactions were assumed to take place between gaseous monatomic components to form all gaseous compounds in the system. In the case of H_2O, for example,

$$2H(g) + O(g) \rightleftarrows H_2O(g) \tag{6}$$

If the free energies of all species in this reaction are known at the temperature of interest, the free energy of reaction, ΔG_r°, can be calculated and used to derive the equilibrium constant, K, where

$$K = P_{H_2O}/P_H^2 \times P_0 \tag{7}$$

assuming, at this low pressure, that the activities of these species are equal to their partial pressures. Thermodynamic data for the gaseous species were obtained from ROSSINI *et al.* (1952), GLASSNER (1957), BREWER and CHANDRASEKHARAIAH (1960), the JANAF Tables (1960 and later), KELLEY (1962), HULTGREN *et al.* (1963), and WICKS and BLOCK (1963).

Using the ideal gas law, equation (7) can be written as

$$N_{H_2O} = KN_H^2 N_O (RT)^2 \tag{8}$$

For each of the 70 species considered, an equation of the same form as (8) can be written and substituted into the 15 mass balance equations. The only variables which then appear in the mass balance equations are the concentrations of the 15 monatomic gaseous components N_H, N_O, N_C, etc. A program was written for an IBM model 360/65 computer in order to solve the mass balance equations for the 15 variables by a rapidly-converging method of successive approximations. When solutions obtained by this technique were substituted into the equations, the left-hand-side of each equation was always within one part in 10^5 of the constant on the right-hand-side.

Equilibrium between a condensed phase and vapor can be represented, in the case of corundum for example, as

$$Al_2O_3(c) \rightleftarrows 2Al(g) + 3O(g) \tag{9}$$

where

$$\log K_{eq} = 2 \log P_{Al} + 3 \log P_0 \tag{10}$$

which assumes that the activities of the gaseous components are equal to their partial pressures. The logarithms of the equilibrium constants, K_{eq}, for such reactions were derived from ΔG_r°'s over the temperature range 1400°K to 1700°K for 75 crystalline phases, many of which are commonly found in meteorites and terrestrial igneous rocks. All condensed phases considered and the sources of their thermodynamic data are listed in Table 2. In most cases, the equation of a straight line through a plot of $\log K_{eq}$ versus $1/T$ was calculated by least squares and was found to give an excellent fit to the data.

The computer generated the concentrations and partial pressures of all components at 2000°K, 1800°K, and 1700°K. At each temperature, and for each condensed phase under consideration the variable K_c was calculated from the partial pressures. In the case of corundum again

$$\log K_c = 2 \log P_{Al} + 3 \log P_0 \tag{11}$$

Table 2. Sources of free energy or vapor pressure data for all crystalline phases considered.

Phase	Source	Phase	Source	Phase	Source	Phase	Source
Fe	2	$Ca_2Mg_5Si_8O_{22}(OH)_2$	3	$FeCl_2$	1	$NaAlSiO_4$	3
Ni	2	Ca_2SiO_4 (larnite)	3	β-SiC	1	$NaAlO_2$	1
Cr	2	$CaSiO_3$ (pseudowollastonite)	3	Si_2N_2O	5	$NaAlSi_2O_6$	3
Mn	2	TiC	1	SiO_2 (quartz)	1	Na_2SiO_3	1
Co	2	TiN	1	α-Si_3N_4	1	$Na_2Si_2O_5$	1
Mg	2	TiO	1	Mg_2Si	1	$Na_4Al_3Si_3O_{12}Cl$	6
Ca	2	Ti_3O_5	1	Mg_2SiO_4	3	Na_2O	1
Na	2	$CaTiO_3$	3	$MgSiO_3$	1*	$KAlSi_3O_8$ (high sanidine)	3
K	2	TiO_2 (rutile)	1	MgO	3	K_2O	3
Al	2	$MgTi_2O_5$	1	$MgCl_2$	1	K_2SO_4	3
Si	1	$CaTiSiO_5$	3	MgF_2	1	KCl	1
Ti	2	$MgTiO_3$	1	$MgCO_3$	3	$KAl_3Si_3O_{10}(OH)_2$	3
C (graphite)	3	$FeTiO_3$	3	$CaCO_3$ (calcite)	3	MnS	3
α-Al_2O_3	3	Ti_2O_3	1	$Ca_3(PO_4)_2$	3	CoO	3
$MgAl_2O_4$	3	Fe_3C	3	CaF_2	1	Cr_2O_3	3
Al_2SiO_5 (kyanite)	1	Fe_3O_4	1	$CaSO_4$	3	MnO	3
$3Al_2O_3{\cdot}2SiO_2$	3	$FeSiO_3$	4	CaO	3	Mn_3O_4	3
$Ca_2Al_2SiO_7$	3	Fe_2SiO_4	3	$CaCl_2$	3	NiO	3
$Ca_3Al_2Si_3O_{12}$	3	FeS	3	Na_2SO_4(I)	1	Mn_2SiO_4	3
$CaAl_2SiO_6$	3	FeS_2	3	$NaAlSi_3O_8$ (high albite)	3	$MnSiO_3$	3
$CaMgSi_2O_6$	3,9	FeO	1	NaCl	1	H_2O	7
$Ca_2MgSi_2O_7$	3	Fe_2O_3	1	NaF	1	CH_4	8
$Ca_3MgSi_2O_8$	3	$MgFe_2O_4$	3	Na_3AlF_6	1	$C_{17}H_{36}$	7

Sources: 1—JANAF Tables (1960 and later)
2—Hultgren *et al.* (1963)
3—Robie and Waldbaum (1968)
4—Larimer (1968)
5—Ryall and Muan (1969)
6—Stormer and Carmichael (1971)
7—Handbook of Chemistry and Physics (1964–1965)
8—Rossini *et al.* (1953)
9—Kracek *et al.* (1953)
*—JANAF Tables, Supplement 3, 1968

where P_{Al} and P_0 are determined by the vapor phase equilibria. For all species the equation of a straight line through a plot of log K_c versus $1/T$ could be calculated. This follows from the linearity of the log of the partial pressure of each component when plotted versus $1/T$, examples of which may be found in the calculations of Russell (1934) and Tsuji (1964).

Treatment of condensed phases

The condition for the presence of a condensed phase is

$$K_c \geq K_{eq} \tag{12}$$

At 2000°K and 1800°K K_c was less than its corresponding K_{eq} for each of the 75 species, but one solid, corundum, was found to be stable by 1700°K. A trial condensation temperature was derived for each phase by simultaneously solving its two linear equations of log K_c and log K_{eq} vs. $1/T$. Corundum was thus found to condense first at 1758°K. Since we assume that each crystalline phase remains in equilibrium with the gas below its condensation point, the previously determined solutions to the equation set at 1700°K are not an accurate representation of the state of the system. At equilibrium K_c cannot be greater than K_{eq}. At 1700°K, the actual P_{Al} must be lower than that determined in the case where no solids were present, since a substantial fraction of the total Al is present as condensed corundum. Thus, for future calculations below 1758°K, a 16th variable, $N_{Al_2O_3}$, the number of moles per liter of solid corundum, must be added to the mass balance equations for oxygen and aluminum. The 16th equation necessary to determine the state of the system is equation (10), the condition that corundum be in chemical equilibrium with the vapor. New solutions were then generated at 1700°K and the same 16 equations were solved at 1600°K. For each of the remaining 74 uncondensed phases, a new log K_c was calculated at these two temperatures. Each of these 74 pairs of points was found to define a straight line which intersected the previous line through the log K_c points for the same phase at a point corresponding to the condensation temperature of corundum, 1758°K.

After condensation of a phase containing a large fraction of the total mass of an element, the equations of log K_c versus $1/T$ for other phases containing that element were normally altered substantially, as were the condensation temperatures of these phases, while the equations for phases which do not contain that element were only rarely changed significantly. The calculations were continued in this manner to ever lower temperatures. Each time a new condensate appeared, a new set of 75 equations relating log K_c to $1/T$ was generated which gave rise to a revised set of condensation temperatures when each was solved simultaneously with its corresponding member of the fixed set of 75 equations relating log K_{eq} to $1/T$. The next phase to condense was the one whose temperature of appearance was the highest of this new set of condensation temperatures. The phase rule was employed to determine if a phase had to disappear when a new one appeared.

Calculations at different total pressures

The condensation temperatures of metallic iron, forsterite and enstatite were calculated at a series of different total pressures. The partial pressures of Fe, Mg and Si at any temperature were calculated by multiplying their partial pressures at $P_{tot} = 10^{-3}$ atm. by the ratio of the new total pressure to 10^{-3}. At a given temperature, the partial pressure of O was found to remain unchanged as the total pressure varied since P_{H_2} and P_{H_2O} always changed by the same factor while the equilibrium ratio $P_{H_2O}/P_{H_2} \times P_O$ had to remain constant. These calculations are consistent with the assumption that the relative proportions of all the major species of each element are constant while the pressure varies at constant temperature. This behavior is demonstrated by the detailed equilibrium calculations of SHIMAZU (1967) at low pressures. The depression of the condensation temperature of enstatite caused by the precipitation of forsterite is unimportant for the purpose of this calculation and consequently has not been considered. The calculation assumes that the crystalline phase assemblage immediately preceding the condensation of Fe and forsterite at any pressure is identical to that at 10^{-3} atm. This is certainly not necessarily the case, since saturated vapor pressure curves for different species are free to intersect one another. The series of calculations at 10^{-3} atm. showed that the condensation temperatures of forsterite and enstatite vary over only about 5° regardless of the identity of the Ca- and Al-bearing phases already condensed or of even the presence or absence of the higher temperature condensates. The only possible complication, then, would be the appearance of a phase containing a major fraction (>20 per cent) of the total Mg and/or Si at a higher temperature than that calculated for the condensation of either forsterite or enstatite. This seems improbable, and the assumption is made that it does not occur over the pressure interval considered. It is similarly assumed that the condensation temperatures of iron are not depressed below the values calculated here by the condensation of a higher temperature phase containing a significant fraction of the total iron. Partial justification of these assumptions is afforded by the fact that there are only a relatively small number of refractory compounds of these elements with elements of approximately equal or greater abundance, all of which have maximum condensation temperatures at least 100° below those of the three phases being considered at 10^{-3} atm.

The variation with temperature of the nickel content of the metallic iron was also calculated at a series of different total pressures from 10^{-2} to 10^{-6} atm. assuming ideal solid solution in the alloy.

Error considerations

Since the least squares fit to log K_c versus $1/T$ is usually accurate to better than 0·1 per cent, the maximum error in condensation temperature due to the numerical scatter is 2–3°. The magnitude of the errors in the condensation temperatures introduced by poorly-determined thermodynamic data is difficult to assess and, in general, is different for each phase. An error of as much as 2 kcal/mole in a ΔG_r°, however, will result in maximum errors in condensation temperatures of about 20° in the 2000° region and 15° in the 1200° region for small ΔG_r°'s. For most phases these temperature errors will be smaller since the relative error in ΔG_r° is usually less than in this case. For a more specific estimate of error due to particular differences in thermodynamic data as well as in elemental abundances, the

reader is referred to the Discussion, where the sources of apparent discrepancies between the condensation temperatures calculated here for iron and forsterite and those calculated by previous workers are examined. Such errors assume major importance if they change the order of stability of phases since a significant part of the future path of condensation may be affected. Such an effect could also arise from failure to consider a high temperature phase containing a major element. The changes produced in these ways would be similar to the differences in condensation sequence calculated for systems of different total pressure (LARIMER, 1967) or of different elemental composition (DONN *et al.*, 1968; GILMAN, 1969).

RESULTS

The temperatures of condensation and disappearance of all phases found to condense in this system are listed in Table 3 in the order of their appearance. The fraction of an element condensed and its distribution between the condensed species is shown in Figs. 1 to 4. The data differ from a previous version of the condensation sequence (CLARK *et al.*, 1972) because we have considered here the effects of solid solution in the gehlenite-akermanite series and we have taken the heat of formation of diopside from KRACEK *et al.* (1953) rather than from ROBIE and WALDBAUM (1968). [Robie and Waldbaum averaged an earlier determination by NEUVONEN (1952) with the data of KRACEK *et al.* (1953). But since Neuvonen is a co-author of the Kracek *et al.* paper, it is reasonable to assume that he would prefer the later determination.]

Table 3. Stability fields of equilibrium condensates at 10^{-3} atmospheres total pressure

Phase		Condensation temperature (°K)	Temperature of disappearance (°K)
Corundum	Al_2O_3	1758	1513
Perovskite	$CaTiO_3$	1647	1393
Melilite	$Ca_2Al_2SiO_7$–$Ca_2MgSi_2O_7$	1625	1450
Spinel	$MgAl_2O_4$	1513	1362
Metallic Iron	(Fe, Ni)	1473	
Diopside	$CaMgSi_2O_6$	1450	
Forsterite	Mg_2SiO_4	1444	
	Ti_3O_5	1393	1125
Anorthite	$CaAl_2Si_2O_8$	1362	
Enstatite	$MgSiO_3$	1349	
Eskolaite	Cr_2O_3	1294	
Metallic Cobalt	Co	1274	
Alabandite	MnS	1139	
Rutile	TiO_2	1125*	
Alkali Feldspar	(Na, K)$AlSi_3O_8$	~1000	
Troilite	FeS	700	
Magnetite	Fe_3O_4	405	
Ice	H_2O	$\leq$200	

* Below this temperature, calculations were performed manually using extrapolated high temperature vapor composition data. In some cases, gaseous species which had been very rare assumed major importance at low temperature (CH_4).

Corundum is the first mineral to appear at 1758°K, followed by perovskite at 1647°K. At 1625°K, corundum begins to react with the gas to form melilite, a mineral which exhibits a complete range of solid solution between pure gehlenite ($Ca_2Al_2SiO_7$) and pure akermanite ($Ca_2MgSi_2O_7$). Assuming ideal solid solution, the first melilite to form contains only about 10^{-2} mole % akermanite. With falling temperature, the ratio of melilite to corundum continually increases as does the akermanite content of the melilite. At 1500°K, the melilite contains

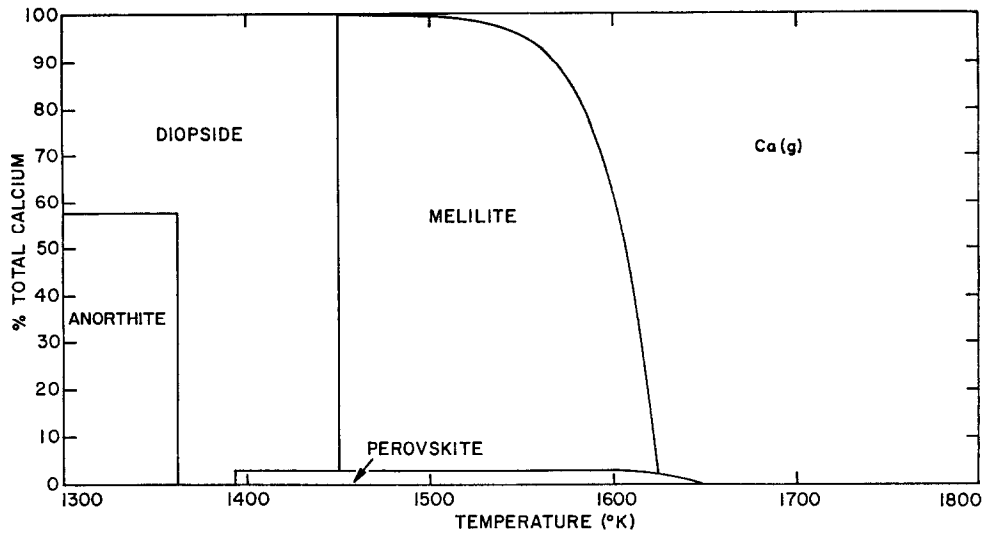

Fig. 1. The distribution of Ca between crystalline phases and vapor. Perovskite condenses at 1647°K, using up only a small fraction of the total Ca. Melilite rapidly consumes most of the Ca soon after appearing at 1625°K. Its Ca is transferred to diopside at 1450°K, when Mg-rich melilite is converted to spinel + diopside. The Ca released when perovskite is converted to Ti_3O_5 at 1393°K is consumed by diopside, which reacts with spinel to form anorthite at 1362°K.

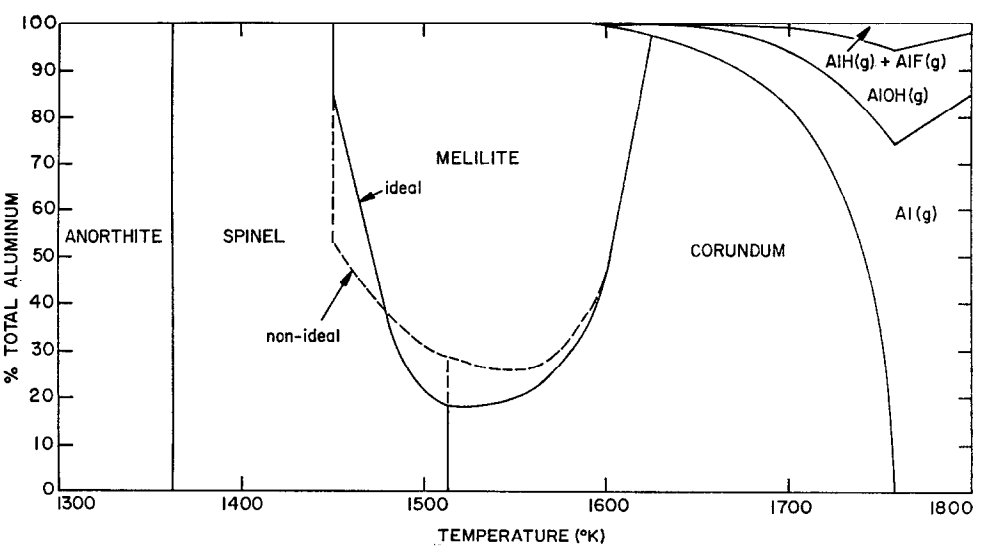

Fig. 2. The distribution of Al between crystalline phases and vapor. Corundum condenses at 1758°K and rapidly consumes most of the Al until it begins to react to form melilite at 1625°K. The ratio of Al in melilite to that in corundum gradually increases with decreasing temperature until 1513°K when the excess corundum is converted to spinel. Below 1513°K, spinel consumes the Al which is displaced from melilite by gaseous Mg. Two sets of curves are shown in this region, one for each melilite solid solution model. The non-ideal model predicts displacement of Al from melilite at temperatures high enough to precipitate corundum. At 1450°K, all the remaining Al in melilite is converted to spinel which is destroyed at 1362°K to form anorthite.

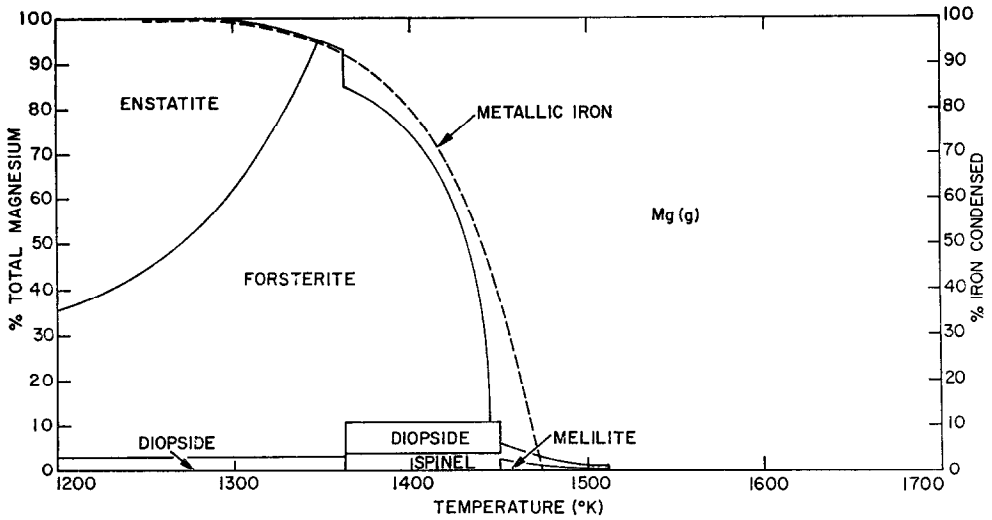

Fig. 3. The distribution of Mg between crystalline phases and vapor. The first Mg-bearing minerals to condense are melilite and spinel, but the fraction of the total Mg contained by them only reaches a few percent by 1450°K where the melilite is destroyed in the production of diopside and more spinel. These curves are drawn for the ideal melilite solid solution model and are almost indistinguishable on this scale from those for the non-ideal case. After forsterite appears at 1444°K, Mg is rapidly condensed with decreasing temperature. At 1362°K diopside reacts with spinel, releasing 8 per cent of the total Mg to forsterite. At 1349°K forsterite begins to react with the gas to form enstatite and the forsterite to enstatite ratio gradually decreases with falling temperature. The condensation curve of metallic Fe is shown for reference. Forty-six per cent of the Fe has condensed before the first appearance of forsterite.

5·7 mole% akermanite and, by 1450°K, 81 mole% akermanite is in ideal solid solution. A more refined estimate is possible by considering to what extent non-ideal solid solution occurs. The existence of a minimum at 72 mole% akermanite in the liquid–solid phase relations of the system gehlenite–akermanite (OSBORN and SCHAIRER, 1941) indicates non-ideal mixing in this series. NEUVONEN (1952) found both positive and negative heats of formation of crystalline melilite solid solutions from pure end members of up to 2 kcal/mole at 25°C. A plot of these excess enthalpies against mole fraction can be fitted to a third order polynomial, the coefficients of which can be used to generate the activity coefficient of each component at any composition and temperature using the regular asymmetric solution model of THOMPSON (1967), if the excess entropy of mixing is assumed to be zero. The mole% akermanite at various temperatures is shown in Table 4 for both solid solution models. Since non-ideal solutions are more stable than ideal ones at low akermanite contents, dilute solutions contain more akermanite in the non-ideal case than in the ideal case. At higher akermanite contents, where positive deviations occur, the reverse is true.

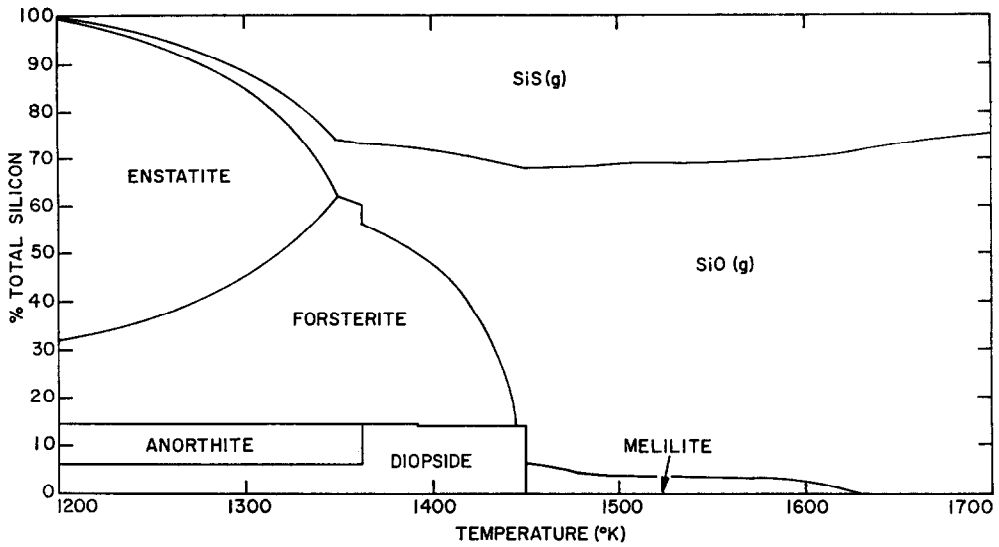

Fig. 4. The distribution of silicon between crystalline phases and vapor. Melilite is the first silicon-bearing phase to condense. The curve shown is for the case of ideal solid solution but the non-ideal curve is very close to this. Less than 15 per cent of the total Si is condensed until forsterite appears at 1444°K. The rate of condensation of Si with falling temperature is further increased below 1349°K where forsterite begins to react with the gas to form enstatite.

Table 4. Variation of the melilite composition with temperature

	Mole % akermanite				
Temperature (°K)	1600	1550	1500	1475	1450
Ideal solid solution	0·02	0·32	5·7	33	81
Non-ideal solid solution	1	7	17	28	43

At 1513°K, corundum is destroyed by reaction with the gas to form spinel. Below 1513°K, when noticeable displacement of Al by Mg takes place in the melilite, the excess Al is consumed in the production of spinel. Using the non-ideal melilite solution model, significant displacement begins in the stability field of corundum so that the excess Al is initially consumed by corundum. Metallic iron first appears at 1473°K and contains 12·1 mole % Ni. As the gas cools and more alloy condenses, its equilibrium Ni content decreases, reaching 4·9 mole %, corresponding to the Ni/Fe ratio of the solar system (CAMERON, 1968), by 1350°K. The akermanite-rich melilite reacts with the gas to form spinel plus diopside at about 1450°K according to both solid solution models. Forsterite first appears at 1444°K, at which temperature 46 per cent of the total iron is already condensed. Perovskite becomes unstable relative to Ti_3O_5 at 1393°K. At 1362°K anorthite forms when spinel is consumed by excess diopside. At 1349°K forsterite begins to react with the gas to form enstatite and the forsterite to enstatite ratio falls smoothly with decreasing temperature as gaseous SiO is consumed.

The fayalite content of the olivine was calculated from the reaction

$$2MgSiO_3(c) + 2Fe(c) + 2H_2O(g) \rightleftarrows Fe_2SiO_4(c) + Mg_2SiO_4(c) + 2H_2(g) \quad (13)$$

using the ratio of enstatite in pyroxene to forsterite in olivine determined experimentally in the presence of iron at 1100°C by LARIMER (1968) and the activity-composition relations for pyroxene at 1250°C and olivine at 1200°C determined by NAFZIGER and MUAN (1967). It is assumed that neither the distribution of iron between olivine and pyroxene nor the activity–composition relations varies greatly from these temperatures to the range 200°C to 600°C. 4·9% Ni was assumed to be in ideal solid solution in the alloy whose composition was assumed to be unaffected by the appearance of troilite at 700°K or by the reactions to form iron-bearing silicates.

Column 2 of Table 5 shows the equilibrium P_{H_2}/P_{H_2O} ratios calculated from the reaction

$$CO(g) + 3H_2(g) \rightleftarrows CH_4(g) + H_2O(g) \quad (14)$$

assuming that the total gaseous oxygen equals the total oxygen in the system minus the oxygen trapped in the equilibrium condensate phase assemblage at 1200°K. Column 3 shows the fayalite contents consistent with these ratios.

Table 5. Equilibrium fayalite content of olivine as a function of temperature in a partially condensed system of solar composition.

Temperature (°K)	P_{H_2}/P_{H_2O}	Mole % fayalite	Range of fayalite contents within error of thermodynamic data
900	1830	0·29	0·18 to 0·50
800	1710	0·51	0·31 to 0·95
700	766	2·2	1·2 to 4·5
600	640	6·8	3·3 to 15
500	640	32	14 to 83

In column 4 are shown the possible ranges of values of the mole% fayalite for an estimated uncertainty of 1·8 kcal/mole in the free energy of reaction (13) which is on the order of only −10 kcal/mole. Similar calculations have been performed by LARIMER (1968) for a comparatively water-rich atmosphere having a $P_{H_2}/P_{H_2O} = 500$. The present data give lower iron contents at each temperatnre due to the more reducing gas considered here.

The first-formed plagioclase is nearly albite-free but will contain 2 mole% albite by 1200°K. The alkali content of the feldspar rises rapidly with decreasing temperature so that pure alkali feldspars are probably stable by 1000°K. Cr_2O_3 becomes stable at 1294°K and metallic Co at 1274°K, assuming that Cr and Co do not form solid solutions with Fe. Cr_2O_3 may also go into solid solution in pyroxene. MnS will condense at 1139°K and Ti_3O_5 will react to form rutile at 1125°K. At 700°K, gaseous H_2S reacts with reduced iron to form FeS. Magnetite will appear below 405°K and ice (H_2O) will not condense until 200°K or less.

The pressure dependence of the condensation temperatures of iron, forsterite and enstatite is shown in Fig. 5. It is clear from this figure that iron has a higher

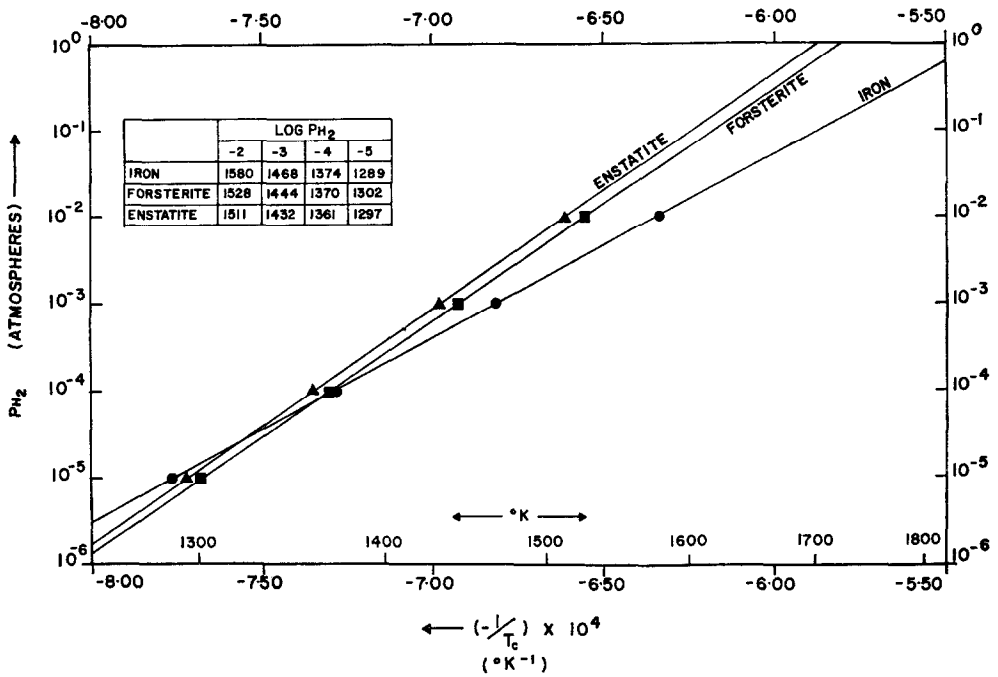

Fig. 5. The variation with pressure of the condensation temperatures of Fe, forsterite and enstatite. The depression of the condensation point of enstatite by the crystallization of forsterite has not been considered in this calculation. At any given pressure, the alloying of Ni in the metal will widen slightly the temperature difference between the appearance of Fe and forsterite. Although this temperature gap is small at 10^{-3} atm., 46 per cent of the Fe will have condensed before forsterite appears.

condensation temperature than forsterite and enstatite at pressures above about $7{\cdot}1 \times 10^{-5}$ atm and $2{\cdot}5 \times 10^{-5}$ atm, respectively. The difference between the temperatures of appearance of iron and forsterite gradually increases with increasing pressure, reaching approximately 80° at 10^{-1} atm. At 10^{-3} atmospheres, 46 per cent of the iron will be condensed before the first appearance of forsterite. Forsterite condenses just before enstatite at all pressures above at least 10^{-6} atm, with the temperature gap between them also gradually increasing with increasing pressure. At 10^{-2} atm, forsterite condenses at 1528°K and enstatite at 1511°K.

Equilibrium condensation of the iron–nickel alloy proceeds in the same fashion over the entire pressure range investigated. The first alloy to condense is relatively nickel-rich but its nickel content rapidly decreases on cooling, with the composition of the alloy always reaching 4·9 mole%, corresponding to the solar Ni/Fe ratio within 150° of its condensation point. In Table 6 are shown the compositions of the first condensing alloys and their condensation points at several different total pressures. Comparison with Fig. 5 indicates an elevation of the condensation temperature of the metal by only 3–5° due to the alloying of nickel. The initial nickel content of the alloy appears to increase very slowly with decreasing pressure, rising 1–1·5 mole% per ten-fold decrease in the total

Table 6. Composition of the first condensing alloy, its condensation temperature, and the fraction of the total iron condensed before the appearance of forsterite as a function of P_{H_2}.

P_{H_2} (atm.)	Condensation temperature of alloy (°K)	Initial nickel content of alloy (mole %)	Fraction of total iron condensed at condensation point of forsterite (%)
10^{-2}	1584	10·9	66
10^{-3}	1473	12·1	46
10^{-4}	1377	13·5	13
10^{-5}	1292	14·9	0
10^{-6}	1218	16·4	0

pressure. The fraction of the total iron condensed at the forsterite condensation temperature appears in column 4 of Table 6. As expected from Fig. 5, increasing the total pressure causes more iron to condense before the appearance of forsterite.

Discussion

Inclusions in the carbonaceous chondrites

Sztrókay *et al.* (1961) noted a white, spinel-bearing nodule in the C2 Kaba. Fredriksson and Reid (1967) reported a gehlenite–spinel intergrowth, 30 μ in diameter, rimmed by gehlenite in a black, carbonaceous fragment in the Sharps chondrite. Subsequently, the assemblage melilite–spinel–perovskite has been observed in numerous C2 and C3 chondrites.

Christophe (1968) described a melilite–spinel chondrule in Vigarano in which the akermanite content of the melilite varies from 40–70 per cent and the spinel is filled with perovskite inclusions. A reaction zone of olivine and spinel was found at the chondrule–matrix contact, into which iron appears to have migrated from the matrix. Spinel-bearing chondrules and spinel–diopside intergrowths containing small amounts of feldspathoids were seen in Lancé and melilite fragments have been observed in Lancé and Felix (Christophe, 1969).

Keil *et al.* (1969) reported achondritic fragments containing spinel, anorthite, perovskite and gehlenite in the C3 Leoville. Reaction zones of spinel were also observed against the carbonaceous chondrite matrix.

Fuchs (1969) has studied achondritic nodules in Allende which contain gehlenite, Ca–Al–Ti clinopyroxene, perovskite, spinel, grossularite, anorthite, aluminous orthopyroxene and an unidentified oxide containing up to 80 per cent Al_2O_3. Many of these phases occur in minute grains from 1–15 μ in size. Sodalite was found in the outer zone of a cordierite-bearing inclusion. Fuchs noted that the common meteoritic silicates, olivine and orthopyroxene, are conspicuously absent from these inclusions.

Marvin *et al.* (1970) estimated that the inclusions in Allende comprise 8 per cent of the meteorite by volume. In addition to the minerals reported by Fuchs (1969), they have identified nepheline and Ca–Al-rich glass in Allende. They noted that spinel is sometimes rimmed by clinopyroxene and is often enclosed by glass. Spinel-bearing patches were also found in the C3 chondrites Grosnaja, Ornans and Warrenton.

In their investigation of the aggregates in Allende, CLARKE *et al.* (1970) determined that the spinel crystals were actually set in a microgranular, nearly isotropic aggregate of gehlenite, anorthite, Ca–Al–Ti pyroxene, and sometimes grossularite and sodalite. Forsterite, never observed in the aggregates, was associated with these minerals only when they formed chondrules. Many aggregates and Ca–Al-rich chondrules were seen to possess narrow reaction rims against the matrix. Their microprobe analysis of a melilite crystal in a chondrule corresponds to 22 mole % akermanite.

In a detailed study of the inclusions in Lancé, KURAT (1970) noted that the cores of the nodules are composed principally of a eutectic-looking intergrowth of spinel and melilite with minor amounts of anorthite, perovskite and Al_2O_3. Diopside invariably rims this phase assemblage. His microprobe analyses of the melilites correspond to 10, 29, 31 and 34 mole % akermanite. Spinel grains in the rims of the inclusions are more Fe-rich (8·4 per cent) than those in the cores (0·8 per cent). To the inside of the diopside rim of one such inclusion, Kurat observed a 2–3 μ wide nepheline-and perovskite-rich zone.

FUCHS *et al.* (1970) reported white inclusions containing spinel and hibonite [$Ca_2(Al, Ti)_{24}O_{38}$] in the C2 Murchison. KEIL and FUCHS (1971) have described spinel–gehlenite–perovskite-bearing inclusions in Leoville and Allende in which hibonite occurs in close contact with spinel or inside spinel grains surrounded by gehlenite.

Melilite is a characteristic mineral of terrestrial impure limestones which have undergone thermal metamorphism in contact zones. It is also found in feldspathoid-bearing rocks which have formed by the reaction of basic magmas with carbonate rocks. Melilite basalts have been studied in many localities, but particularly in the Kola Peninsula, USSR; Iron Hill, Colorado; Uganda and Hawaii. Melilite from basaltic igneous rocks always contains at least 2·75 per cent Na_2O and 0·2 per cent K_2O and often reaches 5 per cent Na_2O and 1·5 per cent K_2O (BERMAN, 1929; GOLDSMITH, 1948; DEER *et al.*, 1962). Its akermanite content is only very rarely less than 35 mole %. The only terrestrial melilites containing less than 0·8 per cent Na_2O and less than 0·2 per cent K_2O occur in contact metamorphic limestones. A significant feature of the meteoritic melilites is their exceptionally low alkali content, 0·2 per cent Na_2O and $<0·05$ per cent K_2O (KURAT, 1970). Many of them exhibit akermanite contents well below 35 mole %. These compositions suggest a chemical history substantially different from that of the relatively alkali-rich, akermanite-rich melilites of igneous rocks. A contact metamorphic origin of the meteoritic inclusions (KEIL and FUCHS, 1971) is considered unlikely, particularly since calcite is extremely rare, if not absent, in the C3's.

MARVIN *et al.* (1970) and LARIMER and ANDERS (1970) noted the similarity of the chemical composition of the mineral assemblage of these aggregates to that of the phases predicted by LORD (1965) to condense from the solar nebula at high temperatures and they included such phases as akermanite and gehlenite among them, by analogy. The data presented here show that, not only are melilite solid solutions expected to condense in the course of cooling of the solar nebula, but also the assemblage spinel–perovskite–melilite is stable in equilibrium

with the vapor over the temperature range 1450° to 1513°K. Above 1513°K, spinel is unstable relative to corundum + vapor. Perhaps the Al_2O_3 reported by KURAT (1970) and the Al_2O_3-rich oxide seen by FUCHS (1969) are relics of this earlier, higher temperature stage. Hibonite is essentially β-Al_2O_3 with up to 20 per cent CaO + TiO_2 + MgO. No thermodynamic data is available for this mineral but Al_2O_3 is the first condensate to appear of those species considered here. The hibonite which KEIL and FUCHS (1971) observed may be the actual mineralogical form of the first Al_2O_3 condensate if it is more stable than corundum in this system above 1758°K. Alternatively, it may be a secondary, low temperature reaction product between corundum, perovskite and melilite. In any case, the presence of this exceedingly Al_2O_3-rich phase in the cores of spinel grains is strongly suggestive of the textural relations expected from the incomplete reaction of corundum with gaseous Mg to form spinel, as predicted above. The eutectic-looking intergrowths of spinel with a melilite containing about 30 mole % akermanite (KURAT, 1970) are easily explained by the fact that, between 1513° and 1450°K, gaseous Mg enters the melilite structure to increase its akermanite content, thereby displacing Al which is immediately precipitated as spinel. The preservation of low-akermanite melilites indicates that the cooling rate was too fast to allow the rapid change in the composition of the melilite expected under equilibrium conditions, although CHRISTOPHE (1968) reported melilites containing 40–70 mole % akermanite. At 1450°K, melilite is converted to a mixture of diopside and spinel, which accounts for the abundant diopside rims around the spinel-melilite intergrowths (KURAT, 1970). The small amount of anorthite in the inclusions may be the product of the later reaction between spinel and diopside at 1362°K. Grossularite may also be a lower temperature reaction product of early-formed condensates. Little thermodynamic data is available for cordierite and it is difficult to determine its position in the condensation sequence. Ca–Al pyroxene is nearly saturated at elevated temperatures in this system and it is not hard to imagine that it could form one component of a solid solution, particularly during slight departures from equilibrium such as incomplete conversion of corundum to spinel or of melilite to diopside plus spinel. Feldspathoids, on the other hand, are never close to saturation in this system over the temperature range investigated. Feldspathoids are not abundant phases in the inclusions and almost always occur interstitially or in the outer margins of the aggregates. This suggests that they may be reaction products between the Al-rich, alkali-poor inclusions and their complementary, relatively Al-poor, alkali-rich carbonaceous chondrite hosts. In the carbonaceous chondrites, Na is mobilized by gentle warming, as suggested by its presence in a hot water extract of Murchison (FUCHS *et al.*, 1970). The reaction rims observed by CLARKE *et al.* (1970) and the demonstration of iron enrichment of the outer zones by CHRISTOPHE (1968) are clear evidence of exchange of matter across the composition contrasts. The coexistence of perovskite and nepheline in one of these border zones seen by KURAT (1970) may indicate a replacement reaction of the form:

$$\underset{\text{from C3 matrix}}{2Na^+} + \underset{\text{solution in pyroxene}}{CaTiAl_2O_6} + \underset{\text{diopside}}{CaMgSi_2O_6} \rightarrow \underset{\text{nepheline}}{2NaAlSiO_4} + \underset{\text{perovskite}}{CaTiO_3} + CaO + Mg^{2+}$$

If chlorine accompanies the incoming Na, sodalite could also form as a reaction product.

Since these inclusions contain no metallic iron or forsterite, it is necessary to postulate that they represent only that fraction of the fine-grained high temperature condensates which had accreted into nodules before the gas temperature had fallen to the condensation point of iron, 1473°K. The existence of diopside rims around the spinel–melilite–perovskite assemblage indicates that agglomeration of these latter phases had taken place above the temperature where diopside appears, which would be 1450°K at a pressure of 10^{-3} atm. The aggregates probably began to accumulate in the median plane of the nebula by gravitational settling soon after condensation upon refractory seed nuclei (CLARK *et al.*, 1972). There they were ultimately joined by iron, olivine, pyroxene, fine-grained lower temperature condensates, chondrules and fragments of other chondritic rock types. The Type III carbonaceous chondrites could form by agglomeration of this mixture.

The lithophile element fractionation in chondrites

LARIMER and ANDERS (1970) have postulated that removal of high temperature condensates from a gas of cosmic composition has produced the lithophile element fractionation observed between the carbonaceous and ordinary chondrites. When the cosmic abundances of CAMERON (1968) are used as the initial composition of the gas, it is found that no combination of phases present in the condensate at 1500°, 1475°, 1450° or 1425°K can be removed from the gas in any proportions to produce a residue having the composition of the ordinary chondrites as long as the distribution of the elements among the condensate phases is constrained to be the equilibrium distribution at the temperature being considered. Larimer and Anders do show, however, that such fractionations can be produced by the removal of various mixtures of specific phases, all of which appear at various temperatures above 1350°K during the course of equilibrium condensation, although never all at once, according to the data presented here. Such a model requires the partial removal of high temperature condensates before they can react to form lower temperature equilibrium phase assemblages. The nodules in the C3 chondrites appear to be likely reservoirs for a fraction of the removed material since they contain mixtures of relict high temperature phases and lower temperature condensates which have only partially replaced them.

The pressure effect on the iron-forsterite condensation sequence

The relative condensation temperatures of iron, forsterite and enstatite may be of extreme cosmochemical and planetological significance. Condensation of iron at a higher temperature than the magnesium silicates has been suggested as a mechanism for at least partial segregation of a growing planet into core and mantle (EUCKEN, 1944; TUREKIAN and CLARK, 1969; CLARK *et al.*, 1972). RINGWOOD (1966) suggested that a metal–silicate separation due to fractional condensation was responsible for the density differences of the planets. Such a process also may have been the cause of the metal–silicate fractionation observed among the ordinary chondrites. A brief examination of the literature, however,

reveals the following inconsistency. WOOD (1963) showed that forsterite condensed at a higher temperature than iron at 10^{-1} atmospheres. LARIMER (1967) claimed that iron condensed before forsterite at $6{\cdot}6 \times 10^{-3}$ atmospheres and ANDERS (1968) stated that forsterite should have appeared before iron at 10^{-4} atmospheres during equilibrium condensation from a cooling gas of cosmic composition. The calculations presented here show that iron condenses at a higher temperature than forsterite at all pressures greater than $7{\cdot}1 \times 10^{-5}$ atm.

It must be emphasized here again that the Fe/Si ratio of 0·89 employed in all these calculations is taken from the cosmic abundance table of CAMERON (1968) who based his value for iron on analyses of the Cl chondrites (WIIK, 1956). For some time, there existed considerable disagreement as to the correct Fe/Si ratio of the solar system. GOLDBERG *et al.* (1960) reported that the Fe/Si ratio of the solar photosphere was 0·12, based on spectroscopic measurements. This cast some doubt on the suggestion that samples having the mean composition of the nonvolatile fraction of solar matter were to be found among the chondritic meteorites (SUESS and UREY, 1956) since this Fe/Si ratio was somewhat less than that derived from analyses of both the H- and L- group chondrites. The first suggestion of misinterpretation of the spectroscopic data was the determination of Fe/Mg in the solar corona by POTTASCH (1963), who gave a value of 1·3 with an error of a factor of two, which agreed with the chondritic abundances. Since then, GARZ and KOCK (1969) have redetermined the oscillator strengths of Fe I and, from this, GARZ *et al.* (1969) suggested a new Fe/H in the photosphere corresponding to an Fe/Si of around 1·0. Using their new measurements of the oscillator strengths of Fe II, BASCHEK *et al.* (1970) calculated photospheric Fe/H ratios which give Fe/Si ratios of 0·7 to 1·75, and NUSSBAUMER and SWINGS (1970) reported a value corresponding to 0·82 based on calculated Fe II oscillator strengths. There seems to be little doubt that the spectroscopic determinations of the iron abundance in the solar corona and photosphere now agree with its measured abundance in the Cl chondrites.

Comparison with previous estimates of condensation points of the major phases

LARIMER (1967) derived the condensation temperature of iron at $6{\cdot}6 \times 10^{-3}$ atm. total pressure, using the vapor pressure curve of BREWER (1946), the data for which appear in BREWER (1950). The measurements quoted by Brewer are taken from the compilation of KELLEY (1935) who, in turn, fitted a curve through the raw data of JONES *et al.* (1927). HULTGREN *et al.* (1963) cite a number of determinations of the vapor pressure curve of iron which have appeared since 1927. They show that the heats of vaporization at 298°K consistent with these later determinations have increased with time, gradually approaching a nearly constant value, almost 3 kcal/mole higher than that from JONES *et al.* (1927), who give the lowest heat of vaporization of all. The condensation temperature of iron determined here, using the data selected by HULTGREN *et al.*, is 40°–50° higher than that of LARIMER (1967) due to the difference between our vapor pressure curves alone. Larimer used the unpublished solar system abundance data of CAMERON (1963a) which gives an Fe/H ratio of $2{\cdot}63 \times 10^{-5}$. Since 1963, Cameron has revised these abundances twice (CAMERON, 1966; 1968). In the latest compilation the Fe/H ratio is $3{\cdot}42 \times 10^{-5}$, 30 per cent higher than that given in 1963. Using the more recent data, the condensation temperature of iron is raised another 10–15° above that of LARIMER (1967). Further discrepancy between our iron condensation temperatures is due to an algebraic error by Larimer.

In the same paper, Larimer reported a condensation temperature for forsterite of 1420°K. This value is 25° less than that reported here, even though the total pressure was a factor of 6·6 higher in his calculation. The Mg/H and Si/H ratios which he used (CAMERON, 1963a) are approximately 20 per cent lower than those used here and this is sufficient to bring the condensation temperature down from 1512°K to about 1501°K at $6{\cdot}6 \times 10^{-3}$ atm. The remaining difference in our estimates (80°) is due to Larimer's use of the H°_{298} for forsterite reported by ROSSINI *et al.* (1952), which is in error by 20 kcal/mole. This error, which does not appear in ROBIE and WALDBAUM (1968), makes forsterite unstable relative to $MgO + SiO_2$ at 1000°K.

ANDERS (1968) reported condensation temperatures for iron and forsterite at 10^{-4} atm total pressure based on new calculations by Larimer. LARIMER and ANDERS (1970), in a footnote, indicate that these values were based on CAMERON'S (1968) abundances and on improved data. His new condensation temperature for iron, 1315°K, is still more consistent with the old vapor pressure curve of BREWER (1946) than with the newer data of HULTGREN *et al.* (1963). His new condensation temperature for forsterite, 1340°K, lies mid-way between that calculated from the thermodynamic data of ROSSINI *et al.* (1952) and that from ROBIE and WALDBAUM (1968).

WOOD (1963) has published condensation temperatures for iron and forsterite over the pressure range 10^{-2} atm. to 10^{5} atm. His condensation temperature for iron at 10^{-1} atm. is 1569°K and that for forsterite is 1629°K. In the present study, iron appears at 1702°K at 10^{-1} atm. Wood has used the Fe/H ratio of GOLDBERG *et al.* (1960) which is a factor of 9·2 lower than that of CAMERON (1968), accounting for approximately 115° of the difference. The remaining difference between our estimates is due to Wood's use of an average of the iron vapor pressure curves of JONES *et al.* (1927), MARSHALL *et al.* (1937), and EDWARDS *et al.* (1951) which results in vapor pressures for iron which are a factor of two higher than those selected by HULTGREN *et al.* (1963). Due to his assumption that essentially all the gaseous oxygen is in the form of H_2O, his condensation temperature for forsterite is 9° higher than that calculated here even though the Mg/H and Si/H ratios of GOLDBERG *et al.* (1960) are lower than those used here by factors of 1·6 and 1·2, respectively.

BLANDER and KATZ (1967) have also reported condensation temperatures for iron and forsterite over a wide range of pressures. At equilibrium, they calculate that iron first appears at 1415°K and forsterite at 1429°K at 10^{-3} atm. They use an Fe/H ratio which is a factor of 3·4 lower than that of CAMERON (1968), resulting in a condensation temperature for iron which is lower than that presented here by about 50°. Their condensation temperature of forsterite is only about 15° lower than that shown here due to their use of Mg/H and SiO/H ratios which are lower by factors of 3·2 and 1·4, respectively, than those consistent with CAMERON (1968).

The Ni content of meteoritic iron

Iron–nickel alloys which condensed from the solar nebula at 10^{-3} atm. total pressure can have Ni contents ranging from 12 mole% to 5 mole%, depending on the temperature at which they ceased to equilibrate with the vapor. Iron meteorites containing less than 5 mole% Ni could have condensed from systems depleted in Ni by removal or incomplete reaction of early-formed, nickel-rich metal (LARIMER and ANDERS, 1970). Since such meteorites are very rare, most metal probably was able to equilibrate with the gas and achieve the minimum Ni content of 5 mole%. Even if 50 per cent of the iron in these alloys later reacted preferentially to form Ni-poor troilite and silicates, the maximum Ni content of the residual alloy would be only 21 mole%, while fully equilibrated alloys would reach only 9·5 mole% Ni. The Ni content of the vast majority of iron meteorites (MASON, 1962) and the metal in the E, H and L group chondrites (MASON, 1965) lies between 5 and 16 mole%, compositions which seem compatible

with this model. Derivation of the Ni-rich irons directly by equilibrium condensation is considered unlikely since alloys of such composition (23–62 weight % Ni) could have condensed only from a nebula whose total pressure was less than 10^{-11} atmospheres. Such pressures for the primitive inner solar system seem unreasonably low for other reasons enumerated by ANDERS (1971).

We have seen that high temperature alloys are more Ni-rich than later ones, a conclusion contrary to the prediction of WOOD (1967), who suggested that the ovoid metal grains in Renazzo were higher temperature condensates than the fine-grained matrix which was more Ni-rich.

Density differences among the terrestrial planets

EUCKEN (1944), TUREKIAN and CLARK (1969), and CLARK *et al.* (1972) have proposed that the earth formed by accretion of material rich in metallic iron followed by material rich in magnesium silicates. This "heterogeneous accumulation" process implies formation of at least part of the Earth's core before forsterite or enstatite have begun to accumulate on the growing planet, unlike other theories of the origin of the Earth (RINGWOOD, 1966). Iron can begin to accumulate before silicates if it condenses first. The data presented here indicate that this is the case for equilibrium condensation from a cooling gas of solar composition at all pressures greater than $7{\cdot}1 \times 10^{-5}$ atmospheres. BLANDER and KATZ (1967), however, have pointed out the existence of considerable barriers to the homogeneous nucleation of iron which might preclude its condensation at the temperatures calculated here. The present discussion assumes that metallic iron nucleates heterogeneously on grains of higher temperature condensates and condenses at its equilibrium condensation point. The iron grains may, in turn, act as nucleation sites for the silicates.

The degree of fractionation of metal from silicate may depend critically on the temperature difference between the condensation points of iron and forsterite and would increase with increasing accretion rate of the iron relative to cooling rate of the gas. If the total pressure in the nebula increased with decreasing distance from the sun (HOYLE and WICKRAMASINGHE, 1968), the temperature gap between the appearance of iron and forsterite would have increased also, in accordance with Fig. 5. UREY (1967) has estimated that the Fe/Si ratio of Mercury is a factor of three greater than that of the Earth and five times that of Mars. This can be understood by applying the heterogeneous accumulation model to a nebula having both pressure and temperature increasing toward the center (CAMERON, 1962). At a pressure on the order of 10^{-1} atmospheres at the radius of Mercury, iron would be nearly completely condensed and forsterite would have just begun to condense at 1600°K. Assuming that the gas density varied across the nebula as T^6 (HOYLE and WICKRAMASINGHE, 1968) and that the pressure at 1 A.U. was 10^{-3} atmospheres, the temperature at this distance from the sun was about 825°K. Sudden dissipation of uncondensed gases at this point could have left Mercury depleted in silicates relative to iron while the Earth might have accumulated not only relatively large quantities of forsterite and enstatite by that time but also a thin veneer of alkali-bearing silicates at that temperature. With a slightly higher dT/dP and/or a higher P and T at

the radius of Mercury, large quantities of water, volatile metals and oxidized iron could have condensed at 1 A.U. as well. Given the above conditions at the radius of Mercury at the time the gas was dissipated, it should be noted that, without a temperature gradient, neither iron nor forsterite would have condensed at 1 A.U. if the pressure there were less than about 10^{-2} atmospheres. The calculation of the variation with time and distance from the sun of the pressure and temperature in the evolving nebula will aid greatly in the determination of the validity of such a model for the origin of compositional differences among the planets. The problem of the extent of iron-silicate fractionation is even more complex than this since it depends not only on the degree of fractional condensation but also on the rate of accretion which is a function of physical conditions which vary with distance from the sun and also on the cooling rate which is a function of temperature and the grain density.

Some consequences of the heterogeneous accretion model will be discussed in a future paper.

Acknowledgments—This work is part of the author's Ph.D. thesis. As advisers, Dr. KARL K. TUREKIAN and Dr. SYDNEY P. CLARK, JR. suggested novel avenues of investigation, critically read the manuscript, and helped clarify several sections of the paper. Their inspiration and advice are gratefully acknowledged.

Drs. P. M. ORVILLE and T. H. BROWN provided helpful advice in the selection and use of thermodynamic data. J. HASBROUCK helped with the computer calculations and Dr. J. R. VAISNYS suggested computer techniques. The hospitality of the Goddard Institute for Space Studies and Dr. S. I. RASOOL in permitting use of the Institute's 360/95 computer for some of the calculations is greatly appreciated. My thanks go to the referees, Drs. J. S. LEWIS, J. W. LARIMER and E. ANDERS for their constructive criticisms. Stimulating and valuable discussions with G. W. BRASS and Drs. J. E. GROVER and A. KATZ are gratefully acknowledged.

REFERENCES

ANDERS, E. (1968) Chemical processes in the early solar system, as inferred from meteorites. *Acc. Chem. Res.* **1**, 289–298.

ANDERS, E. (1971) Meteorites and the early solar system. *Ann. Rev. Astron. Astrophys.* **9**, 1–34.

ARRHENIUS, G. and ALFVÉN, H. (1971) Fractionation and condensation in space. *Earth Planet. Sci. Lett.* **10**, 253–267.

BASCHEK, B., GARZ, T., HOLWEGER, H. and RICHTER, J. (1970) Experimentelle Oszillatorenstärken von Fe II-Linien und die solare Eisenhäufigkeit. *Astron. Astrophys.* **4**, 229–233.

BERMAN, H. (1929) Composition of the melilite group. *Amer. Mineral.* **14**, 389–407.

BLANDER, M. (1971) The constrained equilibrium theory: Sulphide phases in meteorites. *Geochim. Cosmochim. Acta* **35**, 61–76.

BLANDER, M. and KATZ, J. L. (1967) Condensation of primordial dust. *Geochim. Cosmochim. Acta* **31**, 1025–1034.

BREWER, L. (1946) Vapor pressure of the elements. Report for the Manhattan Project MDDC-438C.

BREWER, L. (1950) The thermodynamic and physical properties of the elements. In *The Chemistry and Metallurgy of Miscellaneous Materials. Thermodynamics* (editor L. L. Quill). National Nuclear Energy Series IV-19B. Paper 3, pp. 13–39. McGraw-Hill.

BREWER, L. and CHANDRASEKHARAIAH, M. S. (1960) Free energy functions for gaseous monoxides. Univ. of Calif. Rad. Lab. Rep. UCRL-8713.

BROWN, H. S. (1949) A table of relative abundances of nuclear species. *Rev. Mod. Phys.* **21**, 625–634.

CAMERON, A. G. W. (1962) The formation of the sun and planets. *Icarus* **1**, 13–69.

CAMERON, A. G. W. (1963a) Nuclear astrophysics. Lecture notes from a course given at Yale University, unpublished.

CAMERON, A. G. W. (1963b) Formation of the solar nebula. *Icarus* **1**, 339–342.

CAMERON, A. G. W. (1966) Abundances of the elements. In *Handbook of Physical Constants* (editor S. P. Clark, Jr.). Geol. Soc. Am. Mem. 97, pp. 7–10.

CAMERON, A. G. W. (1968) A new table of abundances of the elements in the solar system. In *Origin and Distribution of the Elements* (editor L. H. Ahrens), pp. 125–143. Pergamon.

CHRISTOPHE, M. (1968) Un chondre exceptionnel dans la météorite de Vigarano. *Bull. Soc. fr. Minéral. Cristallogr.* **91**, 212–214.

CHRISTOPHE, M. (1969) Etude minéralogique de la chondrite CIII de Lancé. In *Meteorite Research* (editor P. M. Millman), pp. 492–499. D. Reidel.

CLARK, S. P. JR., TUREKIAN, K. K. and GROSSMAN, L. (1972) Model for the early history of the earth. In *The Nature of the Solid Earth* (editor E. C. Robertson), pp. 3–18. McGraw-Hill.

CLARKE, R. S. JR., JAROSEWICH, E., MASON, B., NELEN, J., GOMEZ, M. and HYDE, J. R. (1970) The Allende, Mexico, meteorite shower. Smithsonian Contrib. Earth Sci. No. 5.

DEER, W. A., HOWIE, R. A. and ZUSSMAN, J. (1962) *Rock Forming Minerals. Vol. I. Ortho- and Ring Silicates.* Longmans, Green.

DONN, B., WICKRAMASINGHE, N. C., HUDSON, J. P. and STECHER, T. P. (1968) On the formation of graphite grains in cool stars. *Astrophys. J.* **153**, 451–464.

EDWARDS, J. W., JOHNSTON, H. L. and DITMARS, W. E. (1951) The vapor pressures of inorganic substances. VII. Iron between 1356°K and 1519°K and cobalt between 1363°K and 1522°K. *J. Amer. Chem. Soc.* **73**, 4729–4732.

EUCKEN, A. (1944) Physikalisch-chemische Betrachtungen über die früheste Entwicklungsgeschichte der Erde. *Nachr. Akad. Wiss. Göttingen*, Math.-Phys. Kl., Heft 1, 1–25.

FIX, J. D. (1970) Some possible components of circumstellar grain material. *Astrophys. J.* **161**, 359–360.

FREDRIKSSON, K. and REID, A. H. (1967) Meteorite investigations by electron microprobe techniques. In *Researches in Geochemistry* (editor P. H. Abelson), Vol. II, pp. 143–169. Wiley.

FUCHS, L. H. (1969) Occurrence of cordierite and aluminous orthoenstatite in the Allende meteorite. *Amer. Mineral.* **54**, 1645–1653.

FUCHS, L. H., JENSEN, K. J. and OLSEN, E. (1970) Mineralogy and composition of the Murchison meteorite. *Meteoritics* **5**, 198.

GARZ, T., HOLWEGER, H., KOCK, M. and RICHTER, J. (1969) Revision der solaren Eisenhäufigkeit und ihre Bedeutung für das Modell der Sonnenphotosphäre. *Astron. Astrophys.* **2**, 446–450.

GARZ, T. and KOCK, M. (1969) Experimentelle Oszillatorenstärken von Fe I- Linien. *Astron. Astrophys.* **2**, 274–279.

GAST, P. W. (1972) The chemical composition of the earth, the moon, and chondritic meteorites. In *The Nature of the Solid Earth* (editor E. C. Robertson), pp. 19–40. McGraw-Hill.

GILMAN, R. C. (1969) On the composition of circumstellar grains. *Astrophys. J.* **155**, L185–L187.

GLASSNER, A. (1957) The thermochemical properties of the oxides, fluorides, and chlorides to 2500°K. Argonne National Laboratory Rep. ANL-5750.

GOLDBERG, L., MÜLLER, E. A. and ALLER, L. H. (1960) The abundances of the elements in the solar atmosphere. *Astrophys. J.* Suppl. **5**, 1–138.

GOLDSMITH, J. R. (1948) Some melilite solid solutions. *J. Geol.* **56**, 437–447.

HANDBOOK OF CHEMISTRY AND PHYSICS (1964–1965). (editor C. D. Hodgman). Chemical Rubber Company, Cleveland, Ohio.

HOYLE, F. and WICKRAMASINGHE, N. C. (1968) Condensation of the planets. *Nature* **217**, 415–418.

HULTGREN, R., ORR, R. L., ANDERSON, P. D. and KELLEY, K. K. (1963) *Selected Values of Thermodynamic Properties of Metals and Alloys.* Wiley.

JANAF Thermochemical Tables (1960 and later) Compiled by the Thermal Research Lab, Dow Chemical Company, Midland, Michigan.

JONES, H. A., LANGMUIR, I. and MACKAY, G. M. J. (1927) The rates of evaporation and the vapor pressures of tungsten, molybdenum, platinum, nickel, iron, copper and silver. *Phys. Rev.* **30**, 201–214.

KEAYS, R. R., GANAPATHY, R. and ANDERS, E. (1971) Chemical fractionations in meteorites-IV. Abundances of fourteen trace elements in L-chondrites; implications for cosmothermometry. *Geochim. Cosmochim. Acta*, **35**, 337–363.

KEIL, K. and FUCHS, L. H. (1971) Hibonite [$Ca_2(Al, Ti)_{24}O_{38}$] from the Leoville and Allende chondritic meteorites. *Earth Planet. Sci. Lett.* **12**, 184–190.

KEIL, K., HUSS, G. I. and WIIK, H. B. (1969) The Leoville, Kansas meteorite: a polymict breccia of carbonaceous chondrites and achondrites. Abstract. In *Meteorite Research* (editor P. M. Millman), p. 217. D. Reidel.

KELLEY, K. K. (1935) Contributions to the data on theoretical metallurgy. III. The free energies of vaporization and vapor pressures of inorganic substances. U.S. Bur. Mines Bull. 383.

KELLEY, K. K. (1962) Contributions to the data on theoretical metallurgy. U.S. Bur. Mines Bull. 601.

KRACEK, F. C., NEUVONEN, K. J., BURLEY, G. and GORDON, R. J. (1953) Thermochemical properties of minerals. Geophys. Lab. Ann. Rept. Director, 69–74.

KURAT, G. (1970) Zur Genese der Ca–Al-reichen Einschlüsse im Chondriten von Lancé. *Earth Planet. Sci. Lett.* **9**, 225–231.

LARIMER, J. W. (1967) Chemical fractionations in meteorites—I. Condensation of the elements. *Geochim. Cosmochim. Acta*, **31**, 1215–1238.

LARIMER, J. W. (1968) Experimental studies on the system Fe–MgO–SiO_2–O_2 and their bearing on the petrology of chondritic meteorites. *Geochim. Cosmochim. Acta* **32**, 1187–1207.

LARIMER, J. W. and ANDERS, E. (1967) Chemical fractionations in meteorites—II. Abundance patterns and their interpretation. *Geochim. Cosmochim. Acta* **31**, 1239–1270.

LARIMER, J. W. and ANDERS, E. (1970) Chemical fractionations in meteorites—III. Major element fractionations in chondrites. *Geochim. Cosmochim. Acta* **34**, 367–387.

LEWIS, J. S. (1969) Observability of spectroscopically active compounds in the atmosphere of Jupiter. *Icarus* **10**, 393–409.

LORD, H. C. III (1965) Molecular equilibria and condensation in a solar nebula and cool stellar atmospheres. *Icarus* **4**, 279–288.

MARSHALL, A. L., DORNTE, R. W. and NORTON, F. J. (1937) The vapor pressure of copper and iron. *J. Amer. Chem. Soc.* **59**, 1161–1166.

MARVIN, U. B., WOOD, J. A. and DICKEY, J. S. JR. (1970) Ca–Al rich phases in the Allende meteorite. *Earth Planet. Sci. Lett.* **7**, 346–350.

MASON, B. (1962) *Meteorites*. Wiley.

MASON, B. (1965) The chemical composition of olivine–bronzite and olivine–hypersthene chondrites. Am. Mus. Nov. No. 2223, 1–38.

NAFZIGER, R. H. and MUAN, A. (1967) Equilibrium phase compositions and thermodynamic properties of olivines and pyroxenes in the system MgO–"FeO"–SiO_2. *Amer. Mineral.* **52**, 1364–1385.

NEUVONEN, K. J. (1952) Thermochemical investigation of the åkermanite–gehlenite series. *Comm. Géol. Finlande Bull.* **158**, 1–50.

NUSSBAUMER, H. and SWINGS, J. P. (1970) [FeII] Magnetic dipole transition probabilities and the problem of the solar iron abundance. *Astron. Astrophys.* **7**, 455–458.

OSBORN, E. F. and SCHAIRER, J. F. (1941) The ternary system pseudowollastonite–akermanite–gehlenite. *Amer. J. Sci.* **239**, 715–763.

POTTASCH, S. R. (1963) The lower solar corona: Interpretation of the ultraviolet spectrum. *Astrophys. J.* **137**, 945–966.

RINGWOOD, A. E. (1966) Chemical evolution of the terrestrial planets. *Geochim. Cosmochim. Acta* **30**, 41–104.

ROBIE, R. A. and WALDBAUM, D. R. (1968) Thermodynamic properties of minerals and related substances at 298.15°K (25.0°C) and one atmosphere (1.013 bars) pressure and at higher temperatures. U.S.G.S. Bull. 1259.

ROSSINI, F. D., PITZER, K. S., ARNETT, R. L., BRAUN, R. M. and PIMENTEL, G. C. (1953) *Selected Values of Physical and Thermodynamic Properties of Hydrocarbons and Related Compounds*. Carnegie Press.

ROSSINI, F. D., WAGMAN, D. D., EVANS, W. H., LEVINE, S. and JAFFE, I. (1952) Selected values of chemical thermodynamic properties. Part I. Tables. National Bureau of Standards Circular 500.

RUSSELL, H. N. (1934) Molecules in the sun and stars. *Astrophys. J.* **79**, 317–342.

RYALL, W. R. and MUAN, A. (1969) Silicon oxynitride stability. *Science* **165**, 1363–1364.

SHIMAZU, Y. (1967) Thermodynamical aspects of formation processes of the terrestrial planets and meteorites. *Icarus* **6**, 143–174.

STORMER, J. C. JR. and CARMICHAEL, I. S. E. (1971) The free energy of sodalite and the behavior of chloride, fluoride and sulfate in silicate magmas. *Amer. Mineral.* **56**, 292–306.

SUESS, H. E. and UREY, H. C. (1956) Abundances of the elements. *Rev. Mod. Phys.* **28**, 53–74.

SZTRÓKAY, K. I., TOLNAY, V. and FÖLDVÁRI-VOGL, M. (1961) Mineralogical and chemical properties of the carbonaceous meteorite from Kaba, Hungary. *Acta Geologica* **7**, 57–103.

THOMPSON, J. B. JR. (1967) Thermodynamic properties of simple solutions. In *Researches in Geochemistry* (editor P. H. Abelson), Vol. 2, pp. 340–361. Wiley.

TSUJI, T. (1964) Abundance of molecules in stellar atmospheres. *Proc. Jap. Acad.* **40**, 99–104.

TUREKIAN, K. K. and CLARK, S. P. JR. (1969) Inhomogeneous accumulation of the earth from the primitive solar nebula. *Earth Planet. Sci. Lett.* **6**, 346–348.

UREY, H. C. (1952) *The Planets*. Yale University Press.

UREY, H. C. (1954) On the dissipation of gas and volatilized elements from protoplanets. *Astrophys. J.* Suppl. 6, **1**, 147–173.

UREY, H. C. (1967) The abundance of the elements with special reference to the problem of the iron abundance. *Quart. J. R. Astron. Soc., Lond.* **8**, 23–47.

WICKS, C. E. and BLOCK, F. E. (1963) Thermodynamic properties of 65 elements—their oxides, halides, carbides and nitrides. U.S. Bur. Mines Bull. 605.

WIIK, H. B. (1956) The chemical composition of some stony meteorites. *Geochim. Cosmochim. Acta* **9**, 279–289.

WOOD, J. A. (1963) On the origin of chondrules and chondrites. *Icarus* **2**, 152–180.

WOOD, J. A. (1967) Chondrites: their metallic minerals, thermal histories, and parent planets. *Icarus* **6**, 1–49.